第 26 卷第 5 期
2010 年 5 月

无 机 化 学 学 报
CHINESE JOURNAL OF INORGANIC CHEMISTRY

Vol.26 No.5
867-874

一个 Salen 型配体及其锌(Ⅱ)和镍(Ⅱ)配合物配位前后晶体结构及波谱的比较

游 伟[1,2] 姚 成*,[1] 黄 伟*,[2]

([1]南京工业大学理学院,南京 210009)

([2]南京大学化学化工学院,南京微结构国家实验室,配位化学国家重点实验室,南京 210093)

摘要:本文报道了一个双 *N*,*O*-双齿席夫碱配体 4,4′,6,6′-四溴-2,2′-(1,2-亚苯基双(次氮基次甲基))双苯酚 H_2L(由 3,5-二溴-2-羟基苯甲醛和 1,2-苯二胺通过席夫碱缩合反应制得)及其单核五配位锌(Ⅱ)和四配位镍(Ⅱ)配合物 **1** 和 **2**(分子式分别为[ZnL(H_2O)]和[NiL])的合成、晶体结构与波谱表征。对它们在过渡金属离子配位前后的分子结构和超分子作用力、核磁共振波谱、紫外可见和荧光光谱方面的差异进行了详细的比较研究。

关键词:3,5-二溴-2-羟基苯甲醛;1,2-苯二胺;席夫碱缩合反应;Salen 型配合物;晶体结构

中图分类号:O614.24+1;O614.81+3 **文献标识码**:A **文章编号**:1001-4861(2010)05-0867-08

A Salen-Type Ligand and Its Zn(Ⅱ) and Ni(Ⅱ) Complexes: Structural and Spectral Comparisons before and after Metal-Ion Complexation

YOU Wei[1,2] YAO Cheng*,[1] HUANG Wei*,[2]

([1]*College of Sciences, Nanjing University of Technology, Nanjing* 210009)

([2]*State Key Laboratory of Coordination Chemistry, Nanjing National Laboratory of Microstructures, School of Chemistry and Chemical Engineering, Nanjing University, Nanjing* 210093)

Abstract: A bis-*N*,*O*-bidentate Schiff-base ligand H_2L, named as 4,4′,6,6′-tetrabromo-2,2′-(1,2-phenylenebis(nitrilomethylidyne))diphenol and condensed from 3,5-dibromo-2-hydroxybenzaldehyde and 1,2-phenylenediamine, and its mononuclear five-coordinate zinc(Ⅱ) and four-coordinate nickel(Ⅱ) complexes [ZnL(H_2O)] and [NiL] (**1** and **2**) have been synthesized and structurally and spectrally characterized. Detailed comparisons were carried out on the differences in their molecular structures and supramolecular interactions, ^{1}H NMR, UV-Vis and fluorescence spectra before and after metal-ion complexation. CCDC: 763677, H_2L; 763678, **1**; 763679, **2**.

Key words: 3,5-dibromo-2-hydroxybenzaldehyde; 1,2-phenylenediamine; Schiff-base condensation; Salen-type metal complexes; crystal structures

In the past decades there has been much interest in Salen-type ligands and their metal complexes because they are representative models for investigations on the active sites of biologically important metal-containing enzymes[1-6]. Similar to their porphyrin analogues, these planar molecular structures can find applications in the supramolecular and material chemistry. Compared with other building blocks, a clear

收稿日期:2010-01-31。收修改稿日期:2010-04-15。

国家重点基础研究发展规划(973 计划)(No.2007CB925101,2006CB806104),国家自然科学基金(No.20871065),江苏省自然科学基金(No.BK2009226)资助项目。

*通讯联系人。E-mail:yaocheng@njut.edu.cn,whuang@nju.edu.cn

第一作者:游 伟,男,26 岁,硕士;研究方向:配位化学。

advantage of these Salen-type compounds is their synthetic accessibility to support the generation of large series of supramolecular building blocks[7-12] since many of the components can be commercially purchased and are available in a variety of structural alterations.

To date there have been only four reports on four metal complexes of ligand H_2L, namely, cerium(Ⅳ)[13], cadmium(Ⅱ)[14], copper(Ⅱ)[15], and zinc(Ⅱ)[16] complexes, but they are merely involved in the structural descriptions. Recently, we have reported a series of macrocyclic and acyclic Schiff-base metal complexes and detailed comparisons were carried out on the differences in their syntheses, spectral characterizations, molecular structures and supramolecular interactions[17-23]. In this paper, we focus on the spectral and structural comparisons for a Salen-type ligand H_2L and its zinc(Ⅱ) and nickel(Ⅱ) complexes **1** and **2** before and after metal-ion complexation, where the bis-*N*,*O*-bidentate Schiff-base ligand was derived from the condensation between 3,5-dibromo-2-hydroxybenzaldehyde and 1,2-phenylenediamine. The three compounds have been characterized by X-ray single-crystal diffraction analyses where versatile interactions in supramolecular level including coordinative bonding, O–H···O, O–H···N, C–H···Br, O–H···Br hydrogen bonding and aromatic π-π stacking play essential roles in forming different frameworks. Moreover, ^{1}H NMR, FTIR, UV-Vis and fluorescence spectra of ligand H_2L, complexes **1** and **2** have been recorded to compare the differences before and after metal-ion complexation.

1 Experimental

1.1 Materials and measurements

3,5-Dibromo-2-hydroxybenzaldehyde and 1,2-phenylenediamine are commercially available from Aldrich and were used as received. All other solvents and reagents were of analytical grade and used without further purification. Elemental analyses (EA) for carbon, hydrogen and nitrogen were performed on a Perkin-Elmer 1400C analyzer. Infrared (IR) spectra (4 000~400 cm^{-1}) were recorded with a Nicolet FTIR 170X spectrophotometer on KBr disks. UV-Vis spectra were recorded with a Shimadzu UV-3150 double-beam spectrophotometer using a Pyrex cell with a path length of 10 mm at room temperature. ^{1}H NMR spectroscopic measurements were performed on a Bruker AM-500 NMR spectrometer, using TMS ($SiMe_4$) as an internal reference at room temperature. Luminescence spectra were recorded on a Hitachi 850 fluorescent spectrophotometer at room temperature (25 ℃).

1.2 Synthesis of bis-*N*,*O*-bidentate Schiff-base ligand H_2L

3,5-Dibromo-2-hydroxybenzaldehyde (0.126 g, 0.45 mmol) dissolved in 20 mL ethanol was added into a 20 mL ethanol solution of 1,2-phenylenediamine (0.022 g, 0.2 mmol). The mixture was stirred at room temperature for 0.5 h and then refluxed for 3 h. The solution was cooled to room temperature and the resulting orange solid was collected, washed by cold ethanol and dried in vacuo. Yield: 0.107 g, 84.6%. Single crystals of ligand H_2L suitable for X-ray diffraction measurement were obtained from the ethanol solution by slow evaporation in air at room temperature. Anal. Calcd. for $C_{20}H_{12}Br_4N_2O_2$ (%): C 38.01, H 1.91, N 4.43, found (%): C 38.10, H 1.84, N 4.48. Main FTIR absorptions (KBr pellets, cm^{-1}): 3 422 (m), 1 612 (vs), 1 583 (s), 1 434 (vs), 1 358 (m), 1 294 (m), 1 203 (m), 1 163 (s), 862 (m), 739 (m), 758 (s), and 689 (m). ^{1}H NMR (DMSO-d_6 ppm): δ: 14.10 (s, 2H, Ar-OH), 8.98 (s, 2H, HC=N), 7.96 (s, 2H, Ar-H), 7.95 (s, 2H, Ar-H), and 7.55~7.49 (m, 4H, Ar-H). UV-Vis in DMF: λ_{max}=426 and 343 nm.

1.3 Syntheses of mononuclear zinc(Ⅱ) and nickel(Ⅱ) complexes [ZnL(H_2O)] and [NiL] (1 and 2)

Complexes **1** and **2** were prepared by the treatment of 1:1 molar ratio of corresponding metal salts $Zn(ClO_4)_2 \cdot 6H_2O$ (0.075 g, 0.2 mmol) or $Ni(CH_3COO)_2 \cdot 4H_2O$ (0.050 g, 0.2 mmol) in 20 mL ethanol and ligand H_2L in 20 mL ethanol. The mixture was refluxed for 2 h and cooled to the room temperature. The resulting solids were collected in the yields of 0.097 g (68%) for **1** and 0.089 g (64.6%) for **2**. Single crystals of **1** and **2** suitable for X-ray diffraction measurement were obtained from the ethanol solutions by slow evaporation in air at room temperature. Characterizations of complex **1**: Anal. Calcd. for $ZnC_{20}H_{11}Br_4N_2O_3$(%): C 33.72, H 1.56, N 3.93, found(%): C 33.78, H 1.60, N 3.87. Main

FTIR absorptions (KBr pellets, cm^{-1}) for **1**: 3 420 (m), 1 614 (vs), 1 582 (s), 1 501 (s), 1 437 (s), 1 317 (m), 1 236 (w), 1 196 (s), 1 148 (s), 864 (m), 748 (s), 708 (m), and 511 (m). ^1H NMR (DMSO-d_6 ppm): δ: 9.01 (s, 2H, HC=N), 7.87 (s, 2H, Ar-H), 7.77 (s, 2H, Ar-H), 7.70 (d, 2H, Ar-H), and 7.45 (m, 2H, Ar-H). UV-Vis in DMF: λ_{max}= 411, 343 and 299 nm. Characterizations of complex **2**: Anal. Calcd. for $NiC_{20}H_{10}Br_4N_2O_2$(%): C 34.88, H 1.46, N 4.07, found(%): C 34.96, H 1.51, N 3.95. Main FTIR absorptions (KBr pellets, cm^{-1}): 3 405 (m), 1 607 (vs), 1 578 (s), 1 450 (s), 1 439 (s), 1 339 (m), 1 200 (s), 1 171 (s), 860 (m), 743 (m), 721 (s), and 548 (m). UV-Vis in DMF: λ_{max}=483, 380 and 318 nm.

1.4 X-ray data collection and solution

Single-crystal samples of ligand H_2L, complexes **1** and **2** were glue-covered and mounted on glass fibers and used for data collection at 291(2) K on a Bruker SMART 1K CCD diffractometer using graphite monochromated Mo $K\alpha$ radiation (λ=0.071 1 nm). The crystal systems were determined by Laue symmetry and the space groups were assigned on the basis of systematic absences using XPREP, and then the structures were solved by direct method and refined by least-squares method on F_{obs}^2 by using the SHELXTL-PC software package[24-26]. All non-hydrogen atoms were refined on F^2 by full-matrix least-squares procedure using anisotropic displacement parameters. Hydrogen atoms were inserted in the calculated positions assigned fixed isotropic thermal parameters at 1.2 times the equivalent isotropic U of the atoms to which they are attached (1.5 times for the oxygen atoms and the methyl groups of acetonitrile) and allowed to ride on their respective parent atoms. The summary of the crystal data, experimental details and refinement results for ligand H_2L, complexes **1** and **2** is listed in Table 1, while selected bond distances and bond angles are given in Table 2. Hydrogen bonding interactions in ligand H_2L, complexes **1** and **2** are shown in Table 3.

CCDC: 763677, H_2L; 763678, **1**; 763679, **2**.

Table 1　Crystal data and structural refinements for ligand H_2L and complexes 1 and 2

Compound	H_2L	**1**	**2**
Empirical formula	$C_{20}H_{12}Br_4N_2O_2$	$ZnC_{20}H_{11}Br_4N_2O_3$	$NiC_{20}H_{10}Br_4N_2O_2$
Formula weight	631.92	712.34	688.59
T / K	291(2)	291(2)	291(2)
Crystal system	Monoclinic	Orthorhombic	Monoclinic
Space group	$P2_1/n$	$Pnma$	$P2_1/n$
a / nm	1.271 4(2)	1.864 7(5)	1.345 9(2)
b / nm	0.774 3(1)	2.445 4(6)	0.825 3(1)
c / nm	2.084 9(3)	0.465 7(1)	1.833 7(2)
β / (°)	98.80(1)		96.52(1)
V / nm^3	2.028 2(4)	2.123 3(9)	2.023 7(4)
Crystal size / mm	0.10×0.10×0.10	0.10×0.10×0.10	0.08×0.08×0.10
Z	4	4	4
D_c / ($Mg\cdot m^{-3}$)	2.07	2.228	2.26
λ(Mo $K\alpha$) / mm^{-1}	7.956	8.71	8.877
F(000)	1 208	1 356	1 312
Absorption correction	Multi-scan	Multi-scan	Multi-scan
Data collected / unique	3 576 / 1 575	1 920 / 686	9 864 / 3 560
Limiting indices	$-13\leqslant h\leqslant 15, -9\leqslant k\leqslant 9, -24\leqslant l\leqslant 20$	$-22\leqslant h\leqslant 21, -27\leqslant k\leqslant 29, -2\leqslant l\leqslant 5$	$-12\leqslant h\leqslant 16, -9\leqslant k\leqslant 9, -21\leqslant l\leqslant 14$
Max. / min. transmission	0.503 4 / 0.448 6	0.476 3 / 0.476 3	0.537 0 / 0.470 5
R_1, wR_2	R_1=0.041 9, wR_2=0.063 5	R_1=0.052 6, wR_2=0.068 4	R_1=0.050 4, wR_2=0.111 6
Goodness of fit on F^2	0.692	0.695	0.770
$\Delta_{(max, min)}$ / ($e\cdot nm^{-3}$)	440 / −590	560 / −870	700 / −760

$R_1=\sum||F_o|-|F_c||\sum|F_o|$, $wR_2=[\sum[w(F_o^2-F_c^2)^2]\sum w(F_o^2)^2]^{1/2}$.

Table 2 Selected bond distances (nm) and angles (°) for ligand H_2L and complexes 1 and 2

			H_2L		
O1-C8	0.136 5(8)	N1-C1	0.140 7(10)	N2-C2	0.141 4(8)
O2-C15	0.134 0(8)	N1-C13	0.127 9(8)	N2-C20	0.129 0(8)
C2-N2-C20	117.9(6)	N2-C2-C1	118.7(6)	O2-C15-C14	124.1(6)
N1-C1-C6	121.5(6)	N1-C13-C7	122.1(6)	N2-C20-C14	121.0(6)
N1-C1-C2	122.8(6)	O2-C15-C16	117.2(7)		
			1		
Zn1-O1	0.200 5(5)	Zn1-O2	0.203 1(7)	Zn1-N1	0.210 5(7)
O1-Zn1-O2	99.1(2)	O2-Zn1-N1	101.7(3)	Zn1-N1-C3	114.1(5)
O1-Zn1-N1	87.9(2)	Zn1-O1-C10	124.1(5)	Zn1-N1-C4	121.9(6)
			2		
Ni1-O1	0.183 4(5)	O1-C8	0.128 2(9)	N2-C2	0.140 7(12)
Ni1-O2	0.184 1(6)	O2-C15	0.131 4(10)	N2-C20	0.129 8(10)
Ni1-N1	0.185 6(7)	N1-C1	0.142 5(11)		
Ni1-N2	0.1847(6)	N1-C13	0.1289(11)		
O1-Ni1-O2	83.6(2)	N1-Ni1-N2	86.1(3)	N2-C2-C3	124.9(8)
O1-Ni1-N1	95.3(3)	C2-N2-C20	122.1(7)	O1-C8-C7	126.0(8)
O1-Ni1-N2	177.9(3)	N1-C1-C2	113.2(8)	O1-C8-C9	119.4(8)
O2-Ni1-N1	178.3(3)	N1-C1-C6	126.7(7)	O2-C15-C14	122.3(8)
O2-Ni1-N2	95.1(3)	N2-C2-C1	115.0(8)	O2-C15-C16	120.3(8)

Table 3 Hydrogen bonding interactions in ligand H_2L and complexes 1 and 2

D–H···A	D-H / nm	H···A / nm	D···A / nm	∠DHA / (°)
H_2L				
O1–H1···O2	0.096	0.237	0.329 8(6)	162.0
O2–H2···N2	0.082	0.186	0.257 3(7)	145.0
1				
O2–H2A···Br2[a]	0.096	0.278	0.350 1(4)	133.0
2				
C10–H10···Br1[b]	0.093	0.290	0.350 5(9)	124.0

Symmetry codes: [a] x, 1/2−y, 1+z; [b] 3/2−x, −1/2+y, 1/2−z.

2 Results and discussion

2.1 Syntheses and spectral characterizations

Both of the bis-*N*,*O*-bidentate Schiff-base ligand and its transition-metal complexes are easily prepared with high yields (Scheme 1). The FTIR spectra of ligand H_2L, complexes **1** and **2** display sharp peaks at 1 612, 1 614 and 1 607 cm^{-1}, respectively, indicative of the presence of Schiff-base C=N double bond units. In the ^1H NMR spectra, the single peak at 14.10 ppm in ligand H_2L is assigned to the phenolic proton, and it disappears after the complexation with zinc(Ⅱ) ion. In addition, slight alterations in the chemical shift of the protons belonging to the Schiff-base and aromatic units are observed.

UV-Vis spectra of ligand H_2L, complexes **1** and **2** in their DMF solutions were recorded to compare the difference before and after metal-ion complexation. As illustrated in Fig.1, the strong absorption bands at 343 nm for ligand H_2L and 343 and 318 nm for complexes **1** and **2** are assigned to the π-π^* transition of the aromatic rings, whereas the intense absorptions at 426,

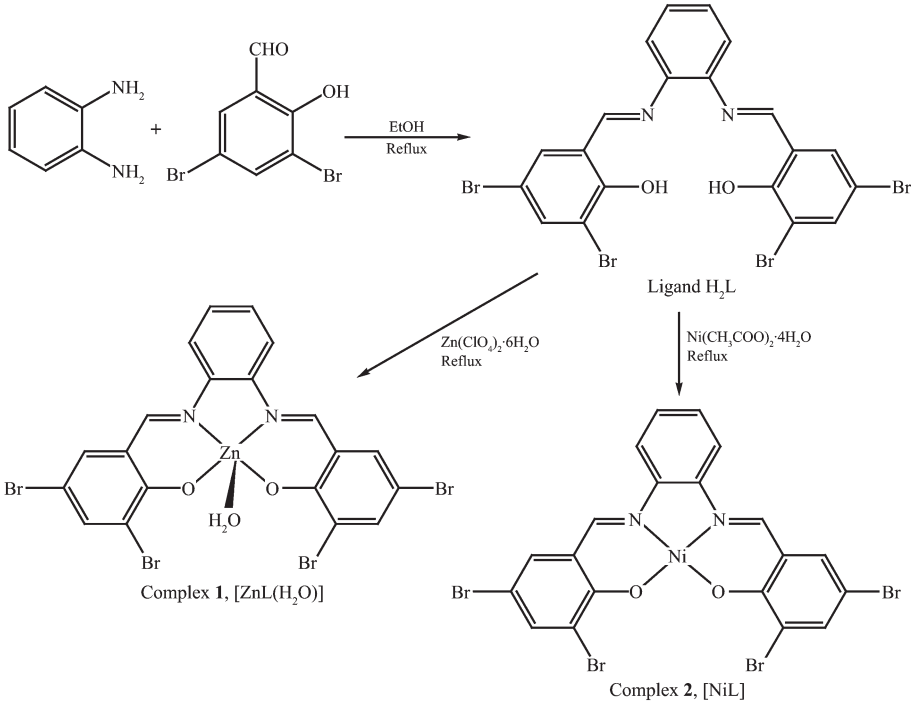

Scheme 1　Schematic illustration for the preparation of ligand H_2L, metal complexes **1** and **2**

411 and 380 nm for ligand H_2L, complexes **1** and **2** are attributed to the π-π* transition of the azomethine chromophore. Furthermore, a new absorption at 483 nm in complex **2** is present corresponding to the typical metal ligand charge transfer transition, which is not observed in the case of complex **1** due to the full d^{10} electronic structure of zinc(Ⅱ) ion.

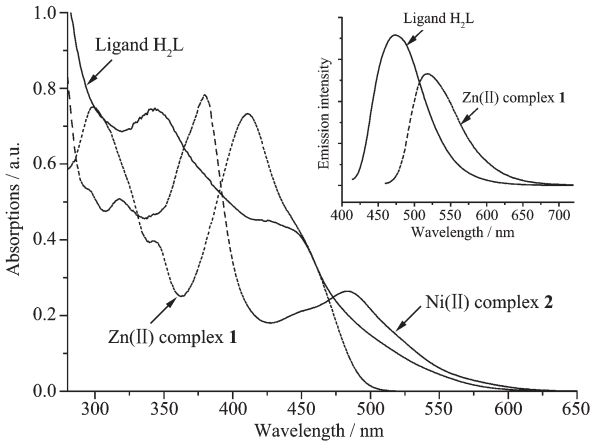

Fig.1　UV-Vis and fluorescence (the inset) spectra of ligand H_2L (solid lines) and its Zn(Ⅱ) (dotted lines) and Ni(Ⅱ) (dashed line) complexes **1** and **2** in their DMF solutions

The inset of Fig.1 gives the fluorescence spectra of ligand H_2L and complex **1** at the same concentration in DMF solutions for comparison. The maximum fluorescence emission band for ligand H_2L and complex **1** exhibits a bathochromic shift of 46 nm from 473 to 519 nm after metal-ion complexation with the zinc(Ⅱ) ion. However, the emission intensity of zinc(Ⅱ) complex is weaker than that of ligand H_2L, which is suggested to originate from the partial fluorescence quench of apically coordinated water molecule in **1**.

2.2　Single-crystal structure of ligand H_2L

The molecular structure of tetradentate Schiff-base ligand H_2L with the atom-numbering scheme is shown in Fig.2. X-ray crystal structural analyses reveal that ligand H_2L crystallizes in the centrosymmetric monoclinic space group $P2_1/n$ and there is only one crystallographically independent molecule in each asymmetric unit without the presence of any solvent molecule. The bond lengths and bond angles in the 3,5-dibromo-2-hydroxybenzaldehyde unit are in the normal range [27]. Every phenyl ring is essentially planar in ligand H_2L, but the dihedral angles between the middle ring (C1 to C6) and the two side rings are 46.6° (C7 to C12) and 14.2° (C14 to C19), respectively. In addition, the two side rings are bended to the opposite direction of the middle ring. Strong intramolecular hydrogen bonds can

be found between one phenolic hydrogen atom and the other phenolic oxygen atom or the Schiff-base nitrogen atom (O1–H1⋯O2 and O2–H2⋯N2) forming an eleven-membered hydrogen-bonded ring.

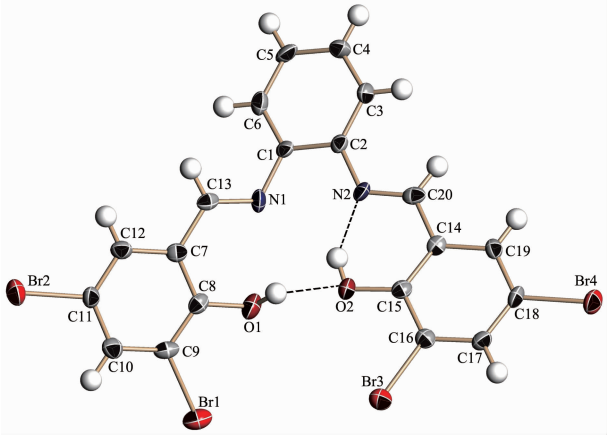

Fig.2 An ORTEP drawing of the Shiff-base ligand H_2L with the atom-numbering scheme, where displacement ellipsoids are drawn at the 30% probability level and the H atoms are shown as small spheres of arbitrary radii

In the packing structure of H_2L, continuous π-π stacking interactions between the middle phenyl ring of one molecule and the side phenolic ring of another adjacent counterpart are found with the centroid-centroid separation of 0.376 1 nm. Thus, a one-dimensional π-π stacking sustained framework is formed, as shown in Fig.3.

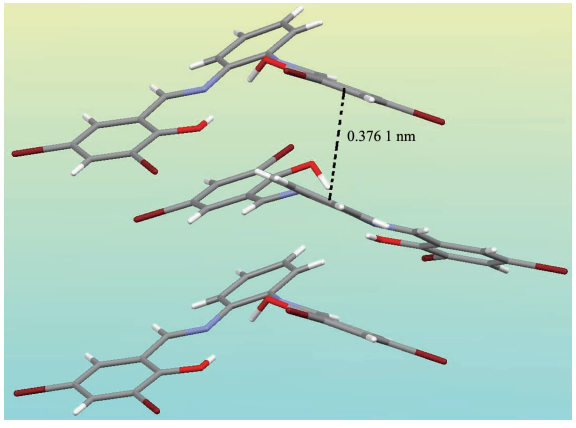

Fig.3 A perspective view of the π-π stacking interactions in the crystal packing of ligand H_2L

2.3 Single-crystal structures of zinc(Ⅱ) complex 1 and nickel(Ⅱ) complex 2

The atom-numbering scheme of complex **1** is shown in Fig.4a, and the X-ray single-crystal diffraction analyses indicate that it crystallizes in the centrosymmetric orthorhombic space group *Pnma*. The central Zn(Ⅱ) ion is five-coordinated by two nitrogen atoms and three oxygen atoms exhibiting distorted pyramidal coordination geometry. Two nitrogen atoms (N1 and N1A, x, 1/2−y, z) and two oxygen atoms (O1 and O1A, x, 1/2−y, z) constitute the basal plane, while another oxygen atom from the coordination water molecule (O2) occupies the apical position. The distance from the central metal ion to the basal least-squares plane is 0.036 7 nm. All the aromatic rings in the ligand are essentially planar, but the dihedral angle between the middle ring and each of the side rings is 20.5°. In the packing structure of **1**, there are two sets of molecules and each set packs in a parallel fashion (Fig.5a) through weak O–H⋯Br intermolecular hydrogen bonding interactions between the hydrogen atom of coordination water molecule and the bromine atom from another

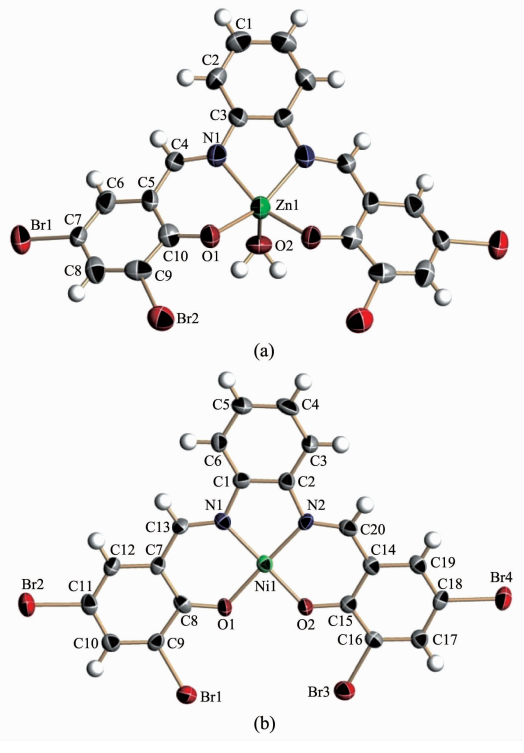

Fig.4 (a) ORTEP drawings of zinc(Ⅱ) complex **1**; (b) nickel(Ⅱ) complex **2** with the atom-numbering scheme, where displacement ellipsoids are drawn at the 30% probability level and the H atoms are shown as small spheres of arbitrary radii

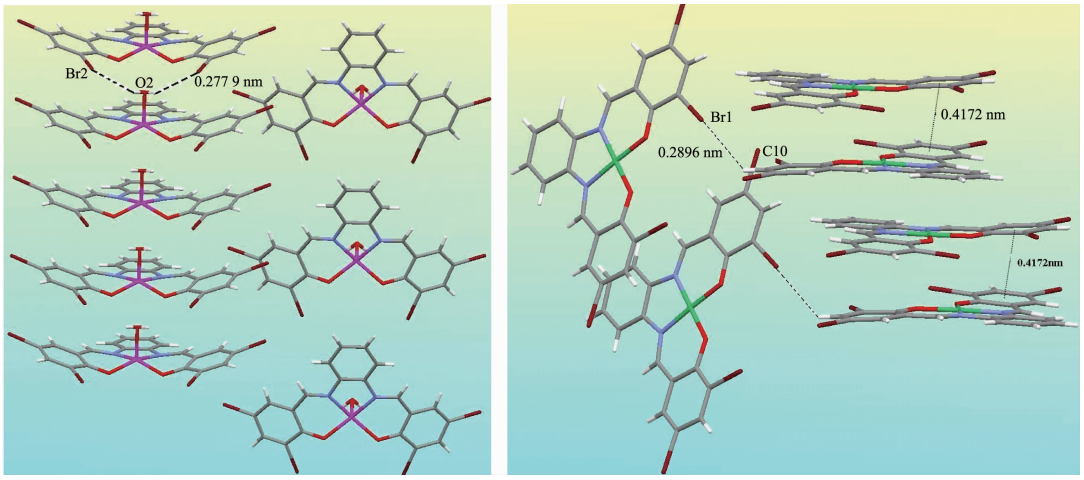

(a)　　(b)

Fig.5　Perspective views of the supramolecular interactions in complexes **1** (a) and **2** (b)

adjacent molecule (Table 3). There is no π-π stacking interaction in the packing mode.

The atom-numbering scheme of complex **2** is shown in Fig.4b, and the X-ray single-crystal structural analyses show it crystallizes in the centrosymmetric monoclinic space group $P2_1/n$ in the absence of any solvent molecule. The nickel(Ⅱ) center is four-coordinated by two Schiff-base nitrogen atoms (N1 and N2) and two phenolic oxygen atoms (O1 and O2) exhibiting slightly distorted square planar coordination geometry with the mean deviation from least-squares plane of 0.001 85 nm. The bond angles of O1-Ni1-N2 and O2-Ni1-N1 are 177.9(3)° and 178.3(3)°, respectively. The bond lengths of N1-C13 and N2-C20 are 0.128 9(11) and 0.129 8(10) nm, while those in ligand H_2L are somewhat shorter (0.127 9(8) and 0.129 0(8) nm) indicative of the influence of metal-ion complexation. Furthermore, the dihedral angels between the middle phenyl ring and the two side aromatic rings in lignad L are very small at 6.2° and 5.6°, respectively, also indicative of the fixation from the square planar coordination plane within molecule.

In the packing structure of **2**, weak offset π-π stacking interactions are found between the side rings of neighboring molecules with the centroid-centroid and interlayer separations of 0.417 2 and 0.342 4 nm (Fig. 5b), respectively. Additionally, weak C−H⋯Br hydrogen bonds between the hydrogen atom of phenyl carbon atom (C10) and its contiguous bromine atom from another molecule (Br1) are observed.

3　Conclusion

In this paper, we have reported the structural and spectral studies on a bis-*N*,*O*-bidentate Schiff base ligand H_2L obtained by the condensation between 3,5-dibromo-2-hydroxybenzaldehyde and 1,2-phenylenediamine, and its mononuclear zinc (Ⅱ) and nickel (Ⅱ) complexes **1** and **2**. Detailed comparisons were carried out on the differences in their molecular and crystal structures, ^{1}H NMR, UV-Vis and fluorescence spectra before and after metal-ion complexation.

References:

[1] Canali L, Sherington D C. *Chem. Soc. Rev.*, **1999**,**28**:85-93
[2] Jacobsen E N. *Acc. Chem. Res.*, **2000**,**33**:421-431
[3] Atwood D A, Harvey M J. *Chem. Soc. Rev.*, **2001**,**101**:37-52
[4] Jacobsen E N, Zhang W, Muci A R, et al. *J. Am. Chem. Soc.*, **1991**,**113**:7063-7064
[5] Katsuki T. *Coord. Chem. Rev.*, **1995**,**140**:189-214
[6] Huang W, Zhu H B, Gou S H. *Coord. Chem. Rev.*, **2006**,**250**: 414-423 and references therein
[7] Sun S S, Stern C, Nguyen S T, et al. *J. Am. Chem. Soc.*, **2004**, **126**:6314-6326
[8] Splan K E, Massari A M, Morris G A, et al. *Eur. J. Inorg. Chem.*, **2003**,**12**:2348-2351
[9] Kitaura R, Onoyama G, Sakamoto H, et al. *Angew. Chem. Int. Ed.*, **2004**,**43**:2684-2687
[10]Huang W, Chu Z L, Gou S H, et al. *Polyhedron*, **2007**,**26**: 1483-1492

[11]Huang W, Chu Z L. *J. Mol. Struct.*, **2007**,**837**:15-22

[12]Azevedo F, Convery M, Domingues D, et al. *Inorg. Chem. Acta*, **1994**,**219**:43-54

[13]Kubono K, Hirayama N, Kokusen H, et al. *Anal. Sci.*, **2001**, **17**:193-197

[14]Shi S M, Song X G, Hu Z Q, et al. *Acta Cryst.*, **2008**,**E64**: m36

[15]Wu Y, Xie B, Zou L K, et al. *Acta Cryst.*, **2009**,**E65**:m758-

[16]Wu Y, Hu Z Q, Li M T, et al. *Acta Cryst.*, **2005**,**E61**:m1352-1353

[17]Chu Z L, Huang W, Wang L, et al. *Polyhedron*, **2008**,**27**:1079-1092

[18]Huang W, Chu Z L, Jiang J C. *Polyhedron*, **2008**,**27**:2705-2709

[19]Wang L, Chu Z L, Huang W, et al. *Inorg. Chem. Commun.*, **2009**,**12**:4-7

[20]Jiang J C, Chu Z L, Huang W. *Inorg. Chim. Acta*, **2009**,**362**: 2933-2936

[21]Chu Z L, You W, Huang W. *J. Mol. Struct.*, **2009**,**920**:277-283

[22]Qian H F, Chu Z L, Huang W. *Chin. J. Inorg. Chem.*, **2009**, **25**:195-200

[23]Fan Y, You W, Huang W, et al. *Polyhedron*, **2010**,**29**:1149-1155

[24]*Siemens, SAINT v*4 *Software Reference Manual, Siemens Analytical X-Ray Systems*, Inc., Madison, Wisconsin, USA, **2000**.

[25]Sheldrick G M. *SADABS, Program for Empirical Absorption Correction of Area Dectector Data*, Univ. of Gottingen, Germany, **2000**.

[26]Sheldrick G M. *SHELXTL, Version* 6.10 *Software Reference Manual, Siemens Analytical X-Ray Systems*, Inc., Madison, Wisconsin, USA, **2000**.

[27]Fan Y, You W, Qian H F, et al. *Acta Cryst.*, **2008**,**E64**:o799